

Preparation of Palladium Composite Membranes on Pore Structure Modified and Non-Modified Supports by Electroless Plating Procedure

Saliha KILIÇARSLAN, Osman Muzaffer AFYON, Meltem DOĞAN*

*Department of Chemical Engineering, Faculty of Engineering & Architecture,
Gazi University, Maltepe, Ankara 06570 TURKEY
e-mail: meltem@gazi.edu.tr*

Received 21.02.2008

The effects of pore structure of the support on the plating morphology, thickness, and composition were investigated in an electroless plating procedure. Some of the plating studies were carried out directly on commercially available porous glass supports, while others were performed on modified supports. Two modification steps with alumina were applied on tubular supports. Formation of a 60- μm -thick layer on the modified support was detected by SEM analysis after the first 2 plating steps, while layer formation was not observed on the non-modified support. It was shown that the formation of a new layer started on the modified support, and a firm structure was obtained on the non-modified support after the fourth plating step. Pd film thickness was 100 μm for plating on the modified support. From EDS analysis, the plating composition on the modified support was 0.52% Al, 1.56% Si, and 97.92% Pd, and it was 2.52% Al, 3.28% Si, and 94.20% Pd on the non-modified support after the fourth plating step. The highest differential gain value was 10.33 mg/cm^2 for the first plating on the modified support. The number of pores corresponding to the mesoporous region increased after the second plating and it decreased with subsequent plating steps for both supports. Pores with an average diameter of about 5500 nm were found in the structure following the fourth plating on the non-modified support, and pores with an average diameter of 800 nm were found basically in the structure after the fourth plating on the modified support.

Key Words: Electroless plating, palladium, composite membrane, support.

Introduction

Palladium and palladium alloyed membranes are suitable for hydrogen separation from gas mixtures and use in reactions such as hydrogenation and dehydrogenation. The techniques generally used in preparing a composite membrane are; nodic oxidation, chemical vapor deposition (CVD), sol-gel, electrolytic plating, and

*Corresponding author

electroless plating. Electroless plating is a very cheap, simple method and it is also applicable on complex shapes. Because of these advantages it is generally preferred. It is based on the auto-catalytic reduction of metallic salt complexes on the surface of the support. Electroless plating conditions (temperature, pH, type of reducing agent, bath composition etc.) directly affect the metal grain size on the surface. Smaller grains form denser films and improve permselectivity; in contrast, larger grains lead to non-selective transport. To prevent large grain formation, it is required to perform studies with lower bath temperatures and adequate precursor supply. Membrane performance is highly relevant to the film thickness; if film thickness is reduced, more hydrogen flux is obtained from the membrane surface. On the other hand, very thin membranes have worse mechanical properties. Dense palladium layers are very selective to hydrogen.^{1,2} Cheng and Yeung³ stated that reducing agents generating hydrogen such as hypophosphite were not suitable for electroless plating of palladium membrane. Altinisik et al.⁴ used a specially designed glass vessel in which helium gas was continuously bubbled through the bath solution to remove hydrogen gas from the surface. It was shown that crack formation due to hydrogen gas was reduced by continuous flow of helium. Palladium deposition progress around the pore area of the support was illustrated by Shi et al.⁵ The observations showed that palladium deposited on the wall of the pores and made a strong palladium “pier”. For long deposition times, a network structure around a pore was built and then palladium formed a thin membrane that fully covered the pore area. Palladium composite membranes were prepared using high velocity oxy-fuel flame spraying (HVOF) and electroless plating by Höllein et al.⁶ It was predicted that thicknesses of the Pd-layers $>3 \mu\text{m}$ (electroless plating) and $>50 \mu\text{m}$ (HVOF) were necessary to obtain defect-free films. The membranes prepared by both preparation methods had a good hydrogen permeability and selectivity combined with sufficient mechanical and thermal stability. Palladium coating on sinter-metal supports using electroless plating was studied by Huang and Dittmeyer.⁷ Zirconia, yttria-stabilized zirconia, and titania were used as porous barriers between the palladium membrane and the sinter-metal support to prevent intermetallic diffusion. All 3 barrier materials and coating methods suppressed the intermetallic diffusion. Osmosis has been used in electroless plating to obtain denser palladium films. It has been observed that using osmosis in electroless plating increases the hydrogen permeability and thermal stability, and membranes have a smaller grain size than conventionally synthesized ones.^{8,9}

It has been predicted that the performance of the Pd membrane and its stability increase by the use of alloys, adding Pd with some other metals like Ag and Cu.^{10–12} Homogeneous Pd-Cu alloy films were obtained by Gao et al.¹³ The composite membranes showed excellent adherence between the alloy layer and the support. Simultaneous deposition of Pd and Ag on the porous alumina tube was achieved using electroless plating by Tanaka et al.¹⁴ The Pd/Ag ratio of the membrane film was controlled in the range of 0-30 wt % by optimizing the chemical composition of the plating solution. Pd and Pd/Ag hollow fiber membranes were synthesized and characterized by Nair et al.^{15,16} Their results showed that robust membranes could be deposited on porous hollow fiber. Pd/Ag membranes exhibited higher permselectivity than Pd membranes.

In the present study, the effects of pore structure of the support on the plating morphology, thickness, and composition were investigated by SEM/EDS analysis. For this purpose some of the plating studies were carried out directly on a commercially available support and the rest were carried out on a support modified with alumina. Changes in the pore size distribution as a result of modification and plating studies were investigated by physisorption and mercury porosimetry analysis.

Experimental

The tubular supports used in the plating studies were purchased from RobuGlasfilter. BET surface area and porosity of original supports were determined as 0.47 m²/g and 0.24, respectively. To obtain a thermal stability on them, supports were subjected to heat treatments twice at 550 °C for 10 h. After heat treatments, BET surface area and porosity values increased to 3.07 m²/g and 0.64, respectively. Pore size distribution curves of the supports before and after the heating procedure are shown in Figure 1, which shows that the pores having diameter in the range of 3-200 nm were open after heat treatments. It was concluded that surface area and porosity were increased because of opened pores. To remove the possible dirt on them, the supports were boiled in 0.1 N NaOH, 0.1 N HCl, and pure water in sequence for 30 min each. The cleaned supports were then dried at 110 °C for 48 h. A porous tube modified with alumina and a non-modified tube were used as supports in the plating studies. To determine the form of alumina that was loaded on the support, firstly aluminum hydroxide (Al(OH)₃) was obtained by the reaction between aluminum nitrate and urea and then it was calcined at 550 °C. The XRD pattern of the alumina synthesized is shown in Figure 2. The peaks at 35.6°, 45.9°, and 66° for the synthesized sample belong to the characteristic peaks of a γ -alumina structure. The supports were then dipped into Al(OH)₃ gel, which was synthesized by the same method mentioned above, and the gel was forced to the surface of the tube by applying a vacuum. Vacuum application on the support took 1 h and following that the support was dried at 120 °C for 24 h. The dried support was heated at 550 °C for 10 h to obtain the transformation of the Al(OH)₃ structure to Al₂O₃. Loading of alumina on the support was repeated with the same vacuum speed. Before plating studies, activation was performed on the modified and non-modified supports. Activation was done by dipping the supports into acidic SnCl₂ solution, acidic PdCl₂ solution, and pure water in sequence for 10 min each. The activation process was repeated 10 times and the solutions were renewed in every step. Before the activation process both sides of the tube were closed with Teflon plugs to prevent the solution coming into contact with the inner surface of the tube. Activation solutions were set so that their volumes would be 0.167 ml for each 1 mm² support surface. Activated supports were then dried at 120 °C for 48 h. Four plating studies were performed on the same support after the activation process. Every plating step took 2 h. The plating bath was prepared such that bath volume would be 0.20 ml for 1 mm² surface for the first 2 plating studies and 0.11 ml for 1 mm² surface for third and fourth plating studies. Performing pre-experiments, the bath composition was selected so that there would be no bulk phase accumulation (Table 1). To prevent bulk phase accumulation, hydrazine was added to the plating bath step by step. For the first 2 platings, 66.7% of total hydrazine was added firstly and the rest was added to the bath between 20 min and 40 min. For the last 2 platings, 33% of the total hydrazine was added first and then 50% of all was added in 30 min; the rest was added to the bath in 60 min during plating studies. Plating studies were carried out at 35 °C and a pH range of 10-11. A schematic representation of the experimental set-up is given in Figure 3. NH₄OH solution was used to adjust pH value at a defined range. After the first plating, the composite structure was dried for 8 days by increasing the temperature from 70 to 120 °C at a rate of 6.25 °C/day. After second plating, the same drying procedure was applied. After the third and fourth platings, drying was carried out at 120 °C for 4 days. After each drying step, differential mass gain was calculated as follows:

$$\text{Differential mass gain} = (\text{WG}_i - \text{WG}_{(i-1)})/A$$

WG_{*i*} : mass of the (substrate + plated palladium) for the *i*th plating step

WG_{*(i-1)*}: mass of the (substrate + plated palladium) for the (*i* - 1)th plating step

A : plated surface area

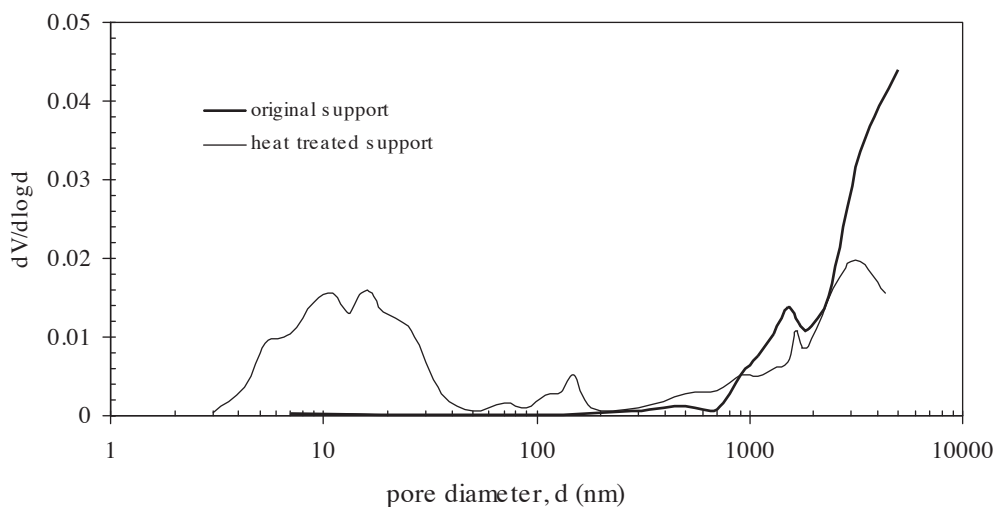


Figure 1. Pore size distribution curves of the supports.

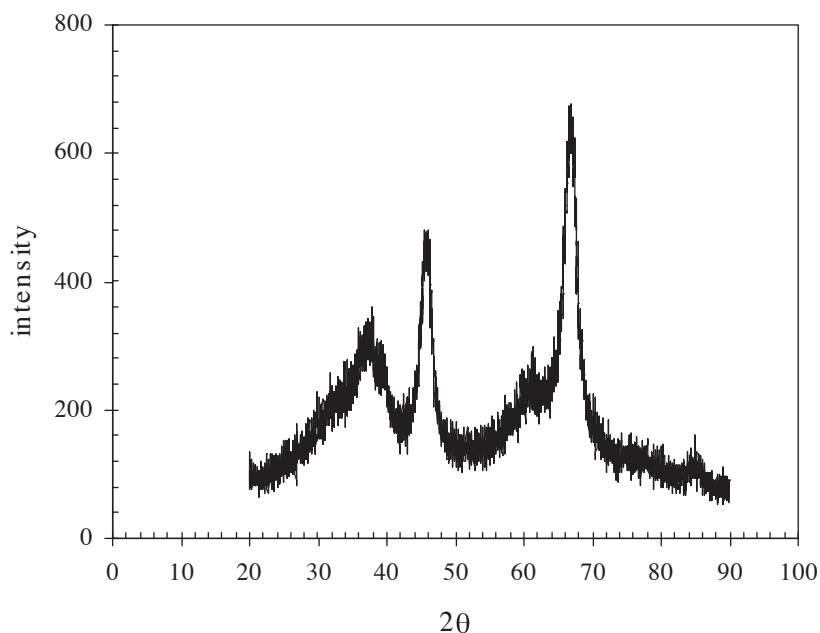


Figure 2. XRD pattern of alumina powder synthesized at 550 °C.

Table 1. Plating bath composition.

PdCl ₂	3.7 g/L
Na ₂ EDTA	7.8 g/L
NH ₄ OH (15 M)	650 mL/L
N ₂ H ₄ (1 M)	15 mL/L

Membrane layer thickness, surface composition, and surface morphology were investigated by SEM/EDS analysis. It was known that there was B (boron) in the structure of the support but it was impossible to detect it by EDS analysis and so all defined compositions in this study were given without B. It was also

investigated how modification and plating studies affected pore size distribution of the supports by using physisorption and mercury porosimetry data.

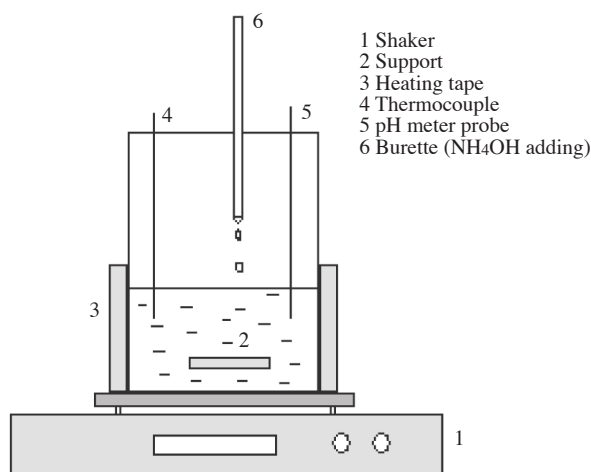


Figure 3. Experimental set-up used in plating studies.

Results and Discussion

Surface SEM photographs of the original and modified support (modified with alumina twice) are given in Figure 4. It can be seen that the pores were filled by alumina after modification. A cross-sectional SEM photograph of the modified support is given in Figure 5, which showed that modification caused an important structural change in the support. The thickness of the region where structural change occurred was $50\ \mu\text{m}$. The thickness of this region was also about $50\ \mu\text{m}$ after the first modification. This result showed that the second modification did not increase the thickness of this region but it gave firmness to the structure. Surface compositions obtained by EDS analysis for the modified (with alumina twice) and non-modified supports are given in Table 2. It is seen that when the Al/Si ratio was 0.057 (by mass) on the non-modified support, it reached a value of 5.65 after 2 modification processes.

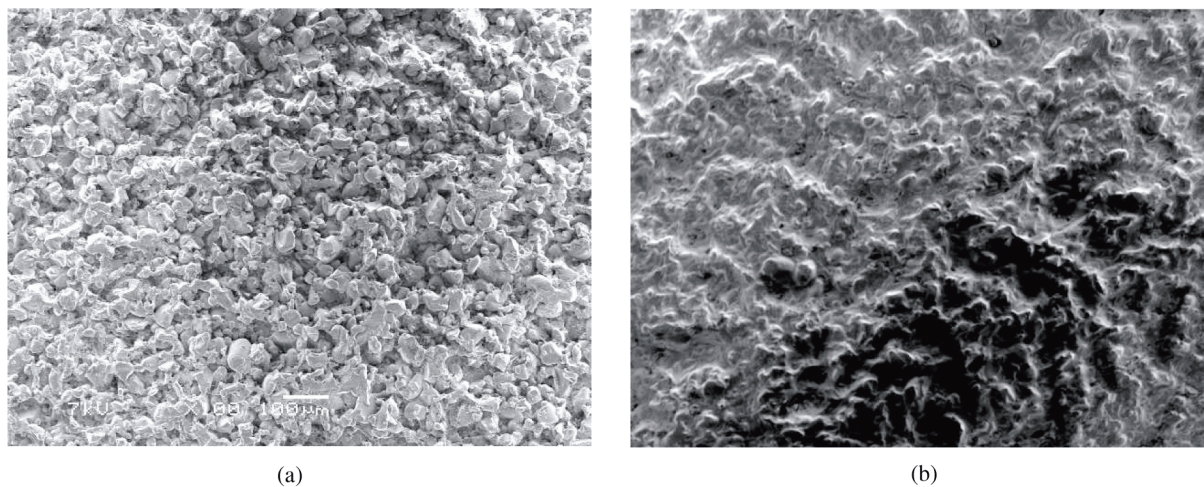


Figure 4. Surface SEM photographs of the supports (a) non-modified (b) modified.

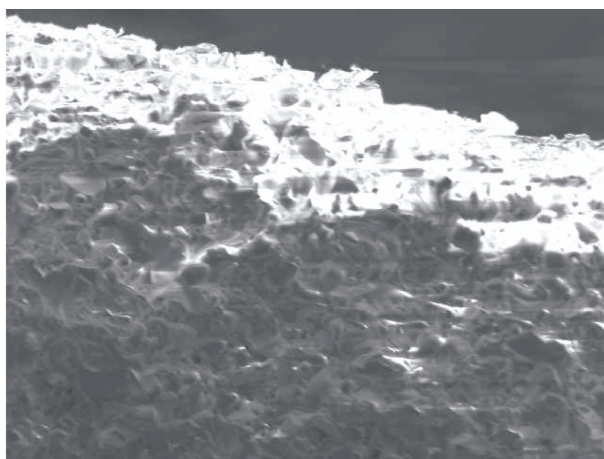


Figure 5. Cross-sectional SEM photograph of the support modified twice with alumina.

Table 2. Surface compositions of the supports (EDS analysis).

element	modified with alumina		non-modified	
	mol (%)	mass (%)	mol (%)	mass (%)
O	83.60	74.62	83.01	72.62
Si	2.13	3.33	12.14	18.65
Al	12.50	18.83	0.72	1.07
Na	1.35	1.73	3.32	4.17
Mg	0.07	0.10	0.10	0.13
Ca	0.01	0.03	0.02	0.03
Fe	0.00	0.00	0.00	0.00
Cl	0.12	0.23	0.04	0.08
Zr	0.22	1.13	0.65	3.25

Before plating studies, activation was performed on the modified and non-modified supports. Surface SEM photographs after activation are given in Figure 6. It is seen that the activation process was performed on a denser surface for the case of the modified support. Surface compositions of the activated surfaces are given in Table 3. The composition determined on an Al, Si, and Pd basis was 6.44% Al, 72.90% Si, and 20.66% Pd on the non-modified support and 45.90% Al, 31.50% Si, and 22.60% Pd for the modified support.

Surface SEM photographs of the plating on the modified and non-modified supports after the first 2 plating steps are given in Figure 7. When surface SEM photographs are compared with each other it can be seen that a dense layer was formed on the modified support. Pd particles started to accumulate on the non-modified support but no such layer was observed. Surface composition determined on an Al, Si, and Pd basis was 0.40% Al, 0.80% Si, and 98.80% Pd for the plating on the modified support. It was 7.70% Al, 3.60% Si, and 88.70% Pd for the plating on the non-modified support. Cross-sectional SEM photographs after the second plating step are given in Figure 8. Three different layers are seen from Figure 8 for plating on the non-modified support: one was a dense layer closer to the surface, another layer was the one in which a structural change occurred after the plating process, and the last one was the support layer. Cross-sectional SEM photographs of the plating on the non-modified support also showed that there

was no film layer formation on the surface. In contrast, it can be seen that a 60- μm film layer formed on the modified support after the first 2 plating procedures.

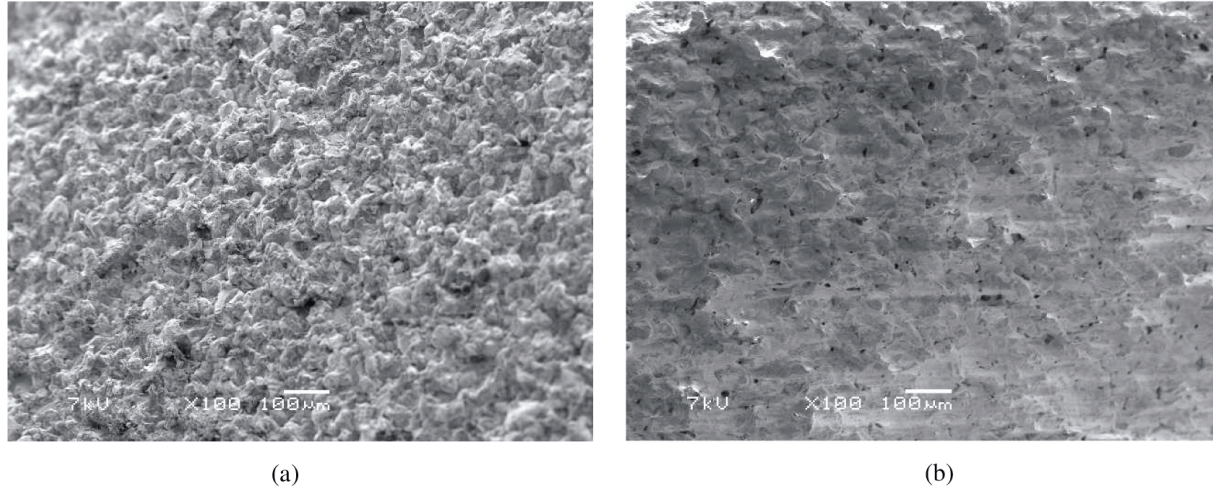


Figure 6. Surface SEM photographs of the activated supports (a) non-modified (b) modified.

Table 3. Surface compositions of the activated supports (EDS analysis).

element	modified support		non-modified support	
	mol (%)	mass (%)	mol (%)	mass (%)
O	80.38	66.45	68.90	51.82
Si	5.96	8.65	20.23	26.71
Al	9.04	12.60	1.86	2.36
Na	1.89	2.25	4.55	4.92
Mg	0.34	0.43	0.07	0.08
Ca	0.43	0.88	0.38	0.72
Fe	0.00	0.00	0.25	0.65
Cl	0.48	0.89	1.70	2.84
Zr	0.35	1.65	0.54	2.33
Pd	1.13	6.20	1.52	7.57

The third and fourth plating steps were carried out on the same supports after the first 2 plating steps. Surface SEM photographs of the composite structures after the fourth plating step are given in Figure 9. When surface photographs after the fourth plating procedure are compared with each other, their surface morphologies appear to be similar. However, if Figures 7 and 9 are evaluated from the same perspective it is possible to say for the plating on the modified support that the formation of a new layer started on the dense layer. Surface composition obtained by EDS analysis on an Al, Si, and Pd basis after the fourth plating process was 0.52% Al, 1.56% Si, and 97.92% Pd for the plating on the modified support. It was 2.52% Al, 3.28% Si, and 94.20% Pd for the plating on the non-modified support. Cross-sectional SEM photographs after the fourth plating step are given in Figure 10. It is seen that plating solution affected approximately 350 μm depth from the surface and caused a structural change in the composite membrane obtained on the non-modified support. A denser layer having a thickness of 85 μm was observed closer to the surface of

that region having a thickness of $350\ \mu\text{m}$. It is also seen from Figure 10 that a membrane layer thickness of $100\ \mu\text{m}$ was obtained for the composite membrane on the modified support. Another cross-sectional SEM photograph of the composite membrane on the modified support shows that there was an excellent adherence between the support and the Pd layer (Figure 11).

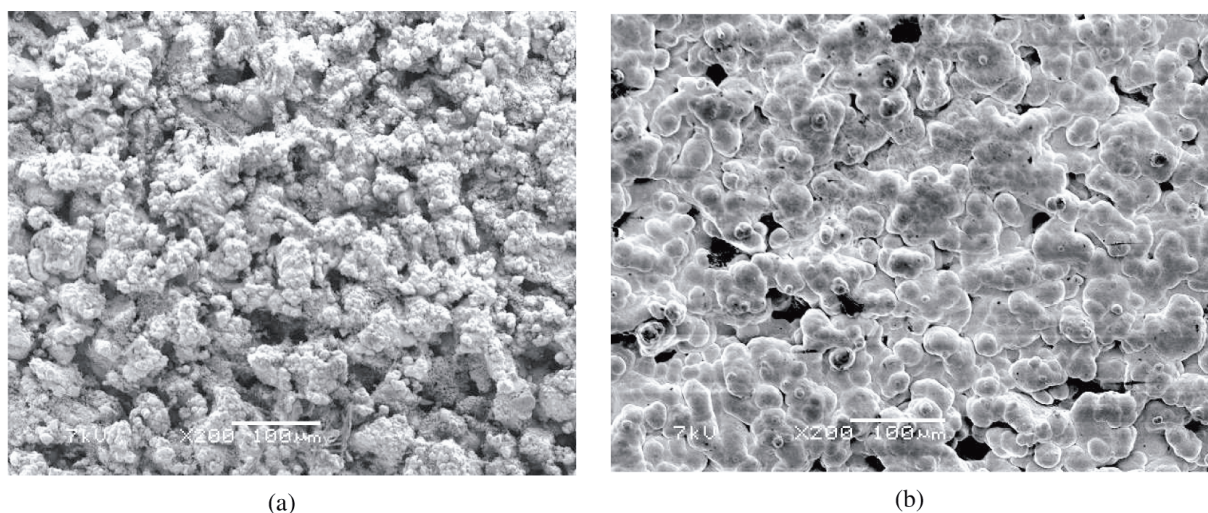


Figure 7. Surface SEM photographs of the platings after the second plating step (a) on non-modified support (b) on modified support.

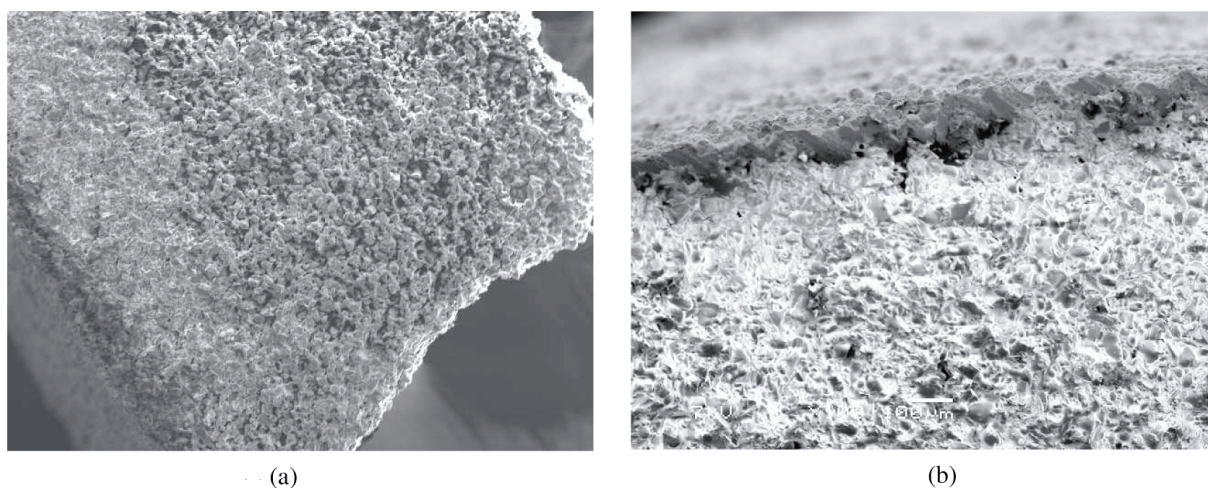


Figure 8. Cross-sectional SEM photographs of the platings after the second plating step (a) on non-modified support ($\times 50$) (b) on modified support ($\times 100$).

It was observed by the SEM/EDS analysis that plating studies on the modified support were more successful than those on the non-modified support. Differential mass gain on the modified support for each plating step is shown in Table 4. The highest differential gain value is $10.33\ \text{mg}/\text{cm}^2$ after the first plating step. Low differential gain values for the plating studies on the non-modified support were determined, even though the maximum value of it was about $4.0\ \text{mg}/\text{cm}^2$.

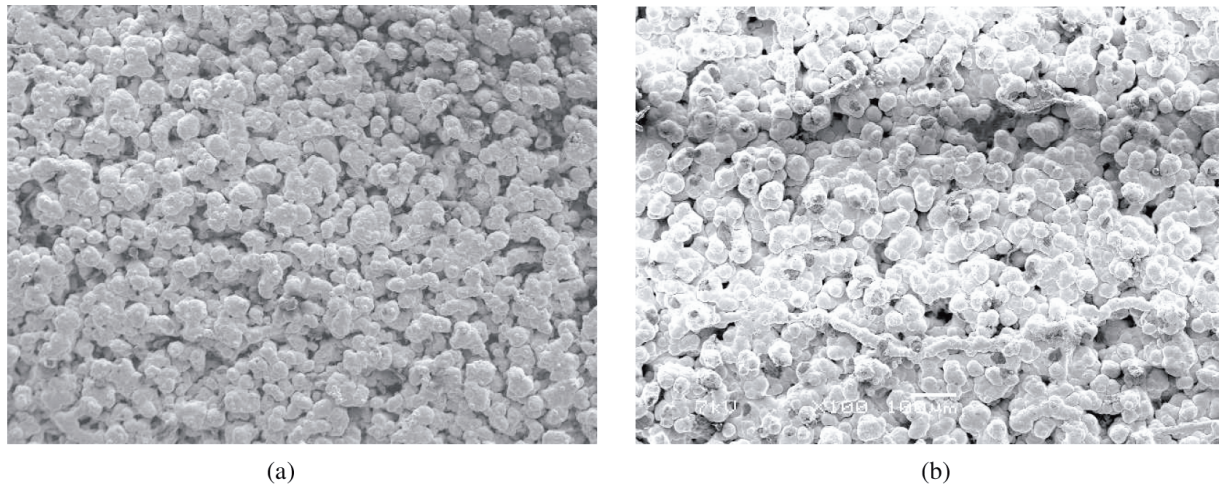


Figure 9. Surface SEM photographs of the platings after the fourth plating step (a) on non-modified support (b) on modified support.

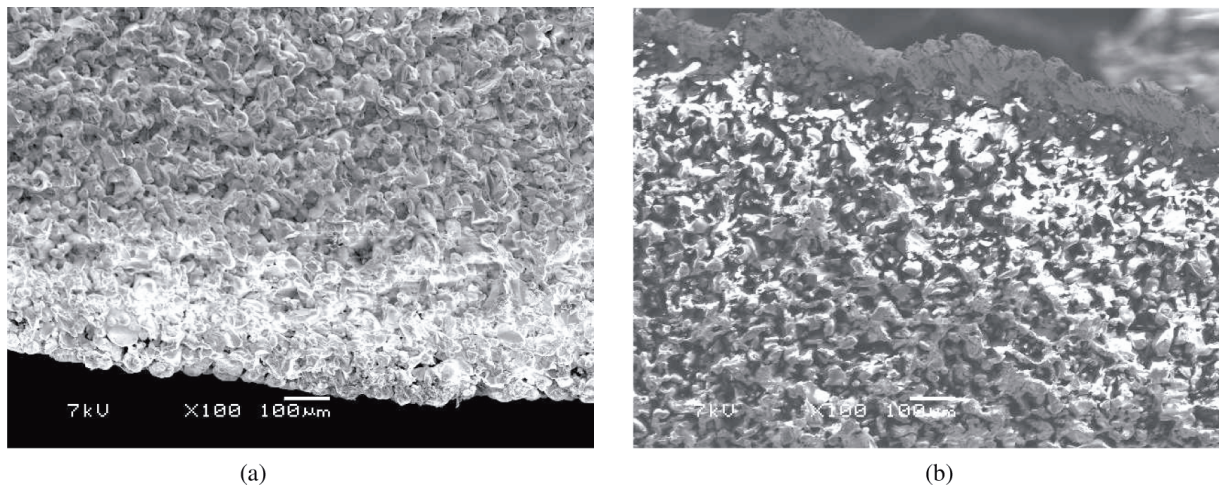


Figure 10. Cross-sectional SEM photographs of the platings after the fourth plating step (a) on non-modified support (b) on modified support.

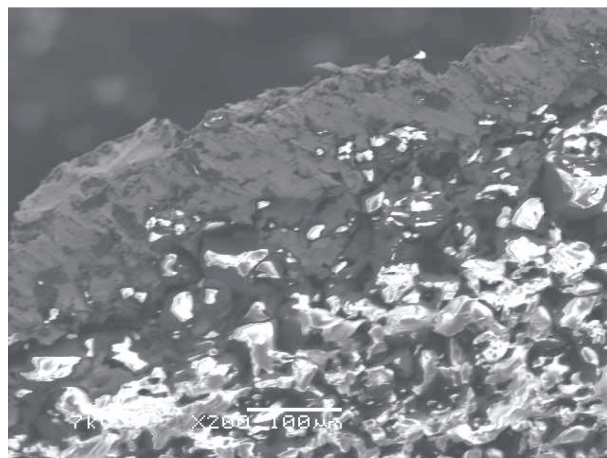


Figure 11. Cross-sectional SEM photographs of the plating on the modified support after the fourth plating step.

Table 4. Differential mass gain values for the plating studies on modified support.

plating number	differential mass gain (mg/cm ²)
1	10.33
2	9.15
3	7.84
4	8.12

Pore size distribution curves are shown in Figure 12 for plating studies on the modified support. While determining the pore size distribution curves, physisorption and mercury porosimetry data were evaluated together. Distribution in the mesoporous region was obtained by the analysis of the nitrogen desorption data according to the BJH method. For the macroporous region, mercury porosimetry data were used. From

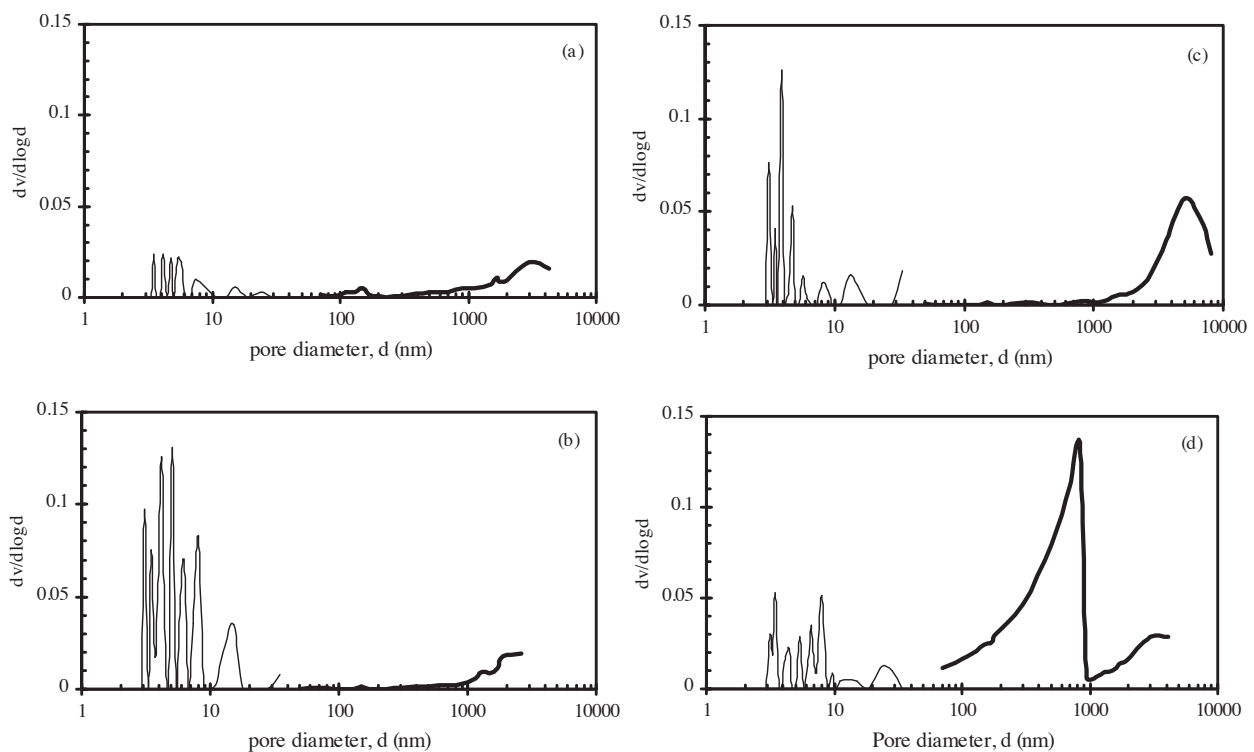


Figure 12. Pore size distribution curves for plating studies on the modified support: (a) support, (b) modified support, (c) composite structure after the second plating step, (d) composite structure after the fourth plating step (— :physisorption, —: mercury porosimeter).

Figure 12, it can be seen that there was harmony between the analysis carried out with different equipment for the mesoporous and macroporous regions. It can be seen that the number of pores with the diameter in the range of 3-20 nm increased after the modification process. After the first 2 plating steps on the modified support, while the number of pores with diameter of about 4 nm did not change significantly, the amount of others decreased in the range of 3-20 nm. After the fourth plating step the number of pores in the mesoporous region decreased sharply and a new distribution curve was formed in the range of 70-1000 nm.

For the plating studies on the non-modified support, it was observed that pores having an average diameter of 4 nm and 10 nm increased after the first 2 plating steps (Figure 13). After the fourth plating step, the pores having diameter range 3-20 nm decreased and there were basically pores with average diameter of 5500 nm in the structure.

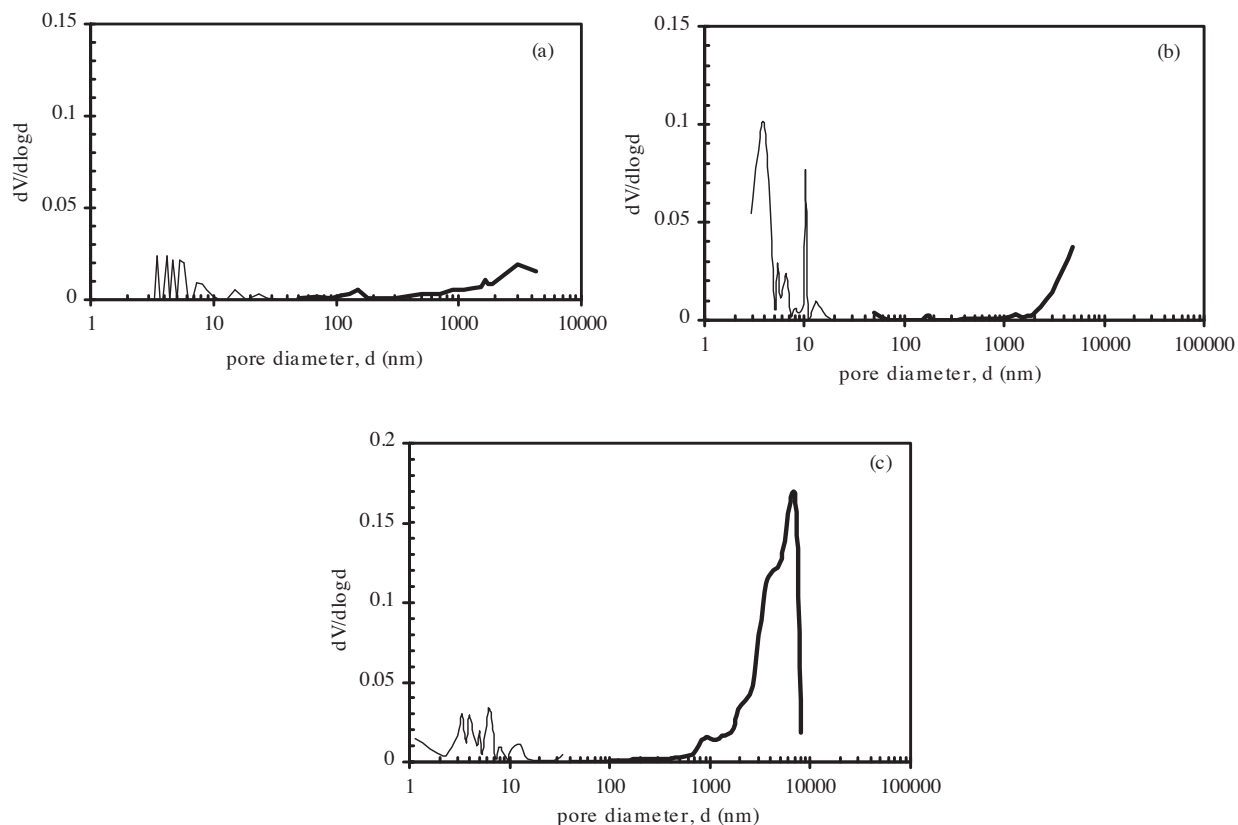


Figure 13. Pore size distribution curves for plating studies on the non-modified support: (a) support, (b) composite structure after the second plating step, (c) composite structure after the fourth plating step (—: physisorption, —: mercury porosimeter).

Conclusions

In this study, palladium was coated on an original porous glass support and a modified support (with alumina twice) by electroless plating technique. Four plating steps having the same operation conditions were performed on both supports. A film layer was formed on the modified support but the formation of a layer was not observed on the non-modified support. It was predicted that the formation of a new layer started on the modified support, and firm plating on the non-modified support was obtained after the fourth plating step. The results of plating studies showed that a membrane layer with the desired properties could be obtained even after the first 2 plating steps on the modified support. Pd film thickness on the modified support was 100 μm after the fourth plating step. The composition obtained on an Al, Si, and Pd basis for the composite membrane on the modified support was 0.52 % Al, 1.56% Si, and 97.92% Pd, and it was 2.52% Al, 3.28% Si, and 94.20% Pd for the composite membrane on the non-modified support. In the studies on both supports, the number of pores corresponding to the mesoporous region increased after the second

plating step. After the fourth plating step, the number of pores in this region decreased while pores in the macroporous region remained basically the same in the structure. This study showed that how the pore size distribution of the support was affected by each plating step will be a significant step in applications of electroless plating on porous supports.

Acknowledgments

The authors are grateful to Professor Gülşen Doğu of Gazi University and Professor Timur Doğu of Middle East Technical University. This work was supported by the Scientific and Technological Research Council of Turkey (Project No: 106M240).

References

1. K. J. Bryden and J. Y. Ying, **Materials Science and Engineering** **204**, 140-145 (1995).
2. V. Jayaraman, Y. S. Lin, M. Pakala and R. Y. Lin, **Journal of Membrane Science** **99** 89-100 (1995).
3. Y. S. Cheng and K. L. Yeung, **Journal of Membrane Science** **182**, 195-203 (2001).
4. O. Altinisik, M. Dogan and G. Dogu, **Catalysis Today** **105**, 641-646 (2005).
5. Z. Shi, S. Wu, J. A. Szpunar and M. Roshd, **Journal of Membrane Science** **280** 705-711 (2006).
6. V. Höllein, M. Thornton, P. Quicker and R. Dittmeyer, **Catalysis Today** **67**, 33-42 (2001).
7. Y. Huang and R. Dittmeyer, **Journal of Membrane Science** **282**, 296-310 (2006).
8. K. L. Yeung, R. Aravind, J. Szegner and A. Varma, **Studies in Surface Science and Catalysis** **101**, 1349 (1996).
9. R. S. Souleimanova, A. S. Mukasyan and A. Varma, **Journal of Membrane Science** **166**, 249-257 (2000).
10. S. Uemiya, T. Matsuda and E. Kikuchi, **Journal of Membrane Science** **56**, 315-325 (1991).
11. Z. Y. Li, H. Maeda, K. Kusakabe, S. Morooka, H. Anzai and S. Akiyama, **Journal of Membrane Science** **78**, 247-254 (1993).
12. S. N. Paglieri and J. D. Way, **Separation and Purification Meth.** **31**, 1-6 (2002).
13. H. Gao, J. Y. S. Lin, Y. Li and B. Zhang, **Journal of Membrane Science** **265**, 142-152 (2005).
14. D. A. P. Tanaka, M. A. L. Tanco, S. Niwa, Y. Wakui, F. Mizukami, T. Namba and T. M. Suzuki, **Journal of Membrane Science** **247**, 21-27 (2005).
15. B. K. R. Nair, J. Choi and M. P. Harold, **Journal of Membrane Science** **288**, 67-84(2007).
16. B. K. R. Nair and M. P. Harold, **Journal of Membrane Science** **290**, 182-195 (2007).